

Random Isotropic Structures and Possible Glass Transitions in Diblock Copolymer Melts

Cheng-Zhong Zhang and Zhen-Gang Wang

*Division of Chemistry and Chemical Engineering,
California Institute of Technology, Pasadena, California 91125*

(Dated: December 2, 2024)

We study the microstructural glass transitions in diblock-copolymer melts using a thermodynamic replica approach. Our approach performs an expansion in terms of the natural smallness parameter – the inverse of the scaled degree of polymerization, which allows us to systematically study the approach to mean-field behavior as the degree of polymerization increases. We find that in the limit of infinite long polymer chains, both the onset of glassiness and the vitrification transition (Kauzmann temperature) collapse to the mean-field spinodal, suggesting that the spinodal can be regarded as the mean-field signature for glass transitions in this class of systems. We also study the order-disorder transitions (ODT) within the same theoretical framework; in particular, we include the leading-order fluctuation corrections due to the cubic interaction in the coarse-grained Hamiltonian, which has been ignored in previous works on the ODT in block copolymers. We find that the cubic term stabilizes both the ordered (body-centered-cubic) phase and the glassy state relative to the disordered phase. While in melts of symmetric copolymers the glass transition always occurs after the order-disorder transition (below the ODT temperature), for asymmetric copolymers, it is possible that the glass transition precedes the ordering transition.

PACS numbers: 61.41.+e, 64.70.Pf, 64.60.My, 64.60.Cn

I. INTRODUCTION

Block copolymers are macromolecules built with blocks of chemically distinct monomers. Melts of block copolymers are attractive from both theoretical and experimental standpoints, as they undergo microphase separations and produce a rich array of ordered microphase structures [1, 2, 3, 4].

The simplest block copolymer is the AB diblock copolymer made of two types of monomers, A and B. Below the order-disorder transition (ODT) temperature, a diblock-copolymer melt can exhibit rich mesophase morphologies [5], including body-centered-cubic (BCC), hexagonally ordered cylinder (HEX), lamellar (LAM), and bicontinuous (*e.g.*, gyroid) structures. Experimentally these structures have been identified using transmission electron microscopy (TEM) [6, 7], small angle neutron scattering (SANS) [6, 8, 9], and dynamic mechanical measurements [8, 9, 10]. Theoretically these structures are well described by the self-consistent-mean-field theory [11, 12].

These periodically ordered structures are generally believed to be equilibrium states [8]. However, they are not easily accessible either in experiments or in computer simulations [8, 13]. Bates *et al.* [3, 8] found that quenching a nearly symmetric diblock-copolymer melt without a symmetry-breaking external field, such as a reciprocal shearing, generally results in isotropic, locally microphase-separated structures with a characteristic length scale of the radius of gyration of the polymer. In addition, such structures were also obtained (as a rule) in the dynamic-density-functional calculations [1, 13, 14]. The ordering kinetics in these random structures are very slow, suggesting that such structures are

metastable states corresponding to free-energy minima. It is therefore quite possible that the periodically ordered phases, though thermodynamically favored, are not easily reached due to the kinetic trapping caused by the presence of a large number of metastable free-energy minima. These metastable states correspond to the locally microphase-separated states without long-range order.

Dynamic mechanical measurements by Bates and coworkers on melts of both symmetric, lamellae-forming [8] and asymmetric, HEX-forming PE-PEP [partially deuterated poly(ethylene-propylene)-poly(ethylene)] copolymers [9] revealed that the system may be frozen in the random structures upon cooling without annealing. Comparing the quenched sample with the slowly supercooled sample and the shear-ordered sample, they found that the quenched sample exhibits very slow relaxations and extraordinarily large elastic moduli at low frequencies; but the supercooled sample behaves more like the disordered melt continuously extended to below the ODT temperature. Balsara and coworkers [15, 16] studied the grain structure of asymmetric, HEX-forming PI-PS (polyisoprene-polystyrene) melt by light scattering, SANS and rheological measurements. Similar to the findings of Bates *et al.*, they found that upon a deep quench, random, locally microphase-separated structures are obtained which do not appear to evolve towards the long-range-ordered equilibrium states within the time scales of the experiments. In addition, randomly oriented wormlike-cylinder structures were found in a I₂S polyisoprene(I)-polystyrene(S) star copolymer system by Gido and coworkers [17].

The above results suggest that the ordering process in block-copolymer melts follow a two-step mechanism: a

fast step in which unlike monomers locally phase separate into random, macroscopically isotropic structures with domains of the size of a single polymer, followed by a domain coarsening (or growth) step in which local defects in the random microstructures annihilate and long-range order develops. The second step is generally much slower than the first and most likely involves thermal-activation processes. Therefore a rapid deep quench can result in a randomly microphase-separated structure, which is kinetically trapped and unable to reach the ordered states which are thermodynamically stable.

This two-step mechanism is in fact consistent with the thermodynamic two-step scenario implicit in the Fredrickson-Helfand (FH) fluctuation theory for diblock-copolymer melts [18] (which is only valid for symmetric or nearly symmetric copolymers.) Instead of the featureless background as assumed in the random-field-approximated structure factor of Leibler [19], the FH theory suggests that when the temperature approaches the ODT, the disordered state be a fluctuating, heterogeneous structure consisting of locally A- and B-rich domains, which then orders into periodic mesophases with long-range order upon further cooling. The most dramatic manifestation of the first step is the existence of the disordered-spherical-micelle state in highly asymmetric copolymer melts, which almost has the appearance of a distinct phase between the featureless disordered phase and the BCC-ordered phase [20, 21, 22, 23, 24, 25, 26, 27]. The micelle state was first predicted by Semenov [28]. Recently Dormidontova and Lodge [29] extended the Semenov theory by including the translational entropy of the disordered spherical micelles and predicted a phase diagram that is in agreement with experiments. More recently, Wang *et al.* [30] examined the nature of the disordered spherical micelles and their connection to concentration fluctuations using the self-consistent-field theory. Taking a nucleation perspective, these authors showed that the disordered micelles are large, localized concentration fluctuations through a thermally activated process.

In this work, we treat these random structures as metastable states and address the possibility of glass transitions in block copolymers using a thermodynamic replica approach. This approach was first proposed by Monasson [31] and subsequently employed by a number of authors in studying structural glasses with self-generated randomness [32, 33, 34, 35, 36, 37]. In this framework the onset of glassiness is attributed to the appearance of an exponentially large number of metastable free-energy minima, which results in a nonvanishing long-time correlation manifested through the cross replica correlation function. An equivalent Kauzmann temperature as in molecular liquids [38] can also be defined here which signals the complete vitrification of the random structures.

The possibility of glasslike transitions in bicontinuous microemulsions – a system closely related to diblock copolymers – was recently examined by Wu *et al.* [39], us-

ing both a dynamic mode-coupling theory and the thermodynamic replica approach. Schmalian, Wolynes, and coworkers have also studied glass transitions in the mathematically isomorphic system of Coulomb-frustrated-magnet using the replica method with a self-consistent-screening approximation [35, 36], and more recently, a local field calculation [37]. Both the microemulsion and the Coulomb-frustrated-magnet systems belong to the general class of models first proposed by Brazovskii [40], featuring the existence of low-energy excitations around some finite wave number q_m and the formation of microphase-separated structures with length scales $\sim 1/q_m$ at low temperatures. These studies showed that as a result of the large degeneracy in the ground states [32], glass transition can occur when the ratio of the correlation length of the system to the modulation length $2\pi/q_m$ exceeds some critical value. Similar conclusions were also obtained by Grousson *et al.* [41] using the mode-coupling theory.

Our work follows a similar approach to that employed by Schmalian, Wolynes, and coworkers [36]. However, we perform calculations specifically for the block-copolymer system by taking advantage of the natural smallness parameter (the inverse of the scaled degree of polymerization \bar{N}); this allows us to systematically examine how the glass transitions are affected by increasing the chain length of the polymer. An important conclusion of our work is that in the limit of infinite long polymers, both the onset of glassiness and the Kauzmann temperature coincide with the mean-field spinodal of the disordered phase. Therefore the spinodal is the mean-field signature for glass transition in these microphase-separating systems. Another feature of our work is the inclusion of the order-disorder transition in the phase diagram. Including the ODT is important because it places the glass transition in the context of the ordering transition. We find that for symmetric, LAM-forming copolymers, the glass-transition temperatures are below the ODT temperature, while for asymmetric, sphere-forming copolymers, the onset of glassiness can precede the ODT into the BCC phase. On a technical point, we provide a method for incorporating the fluctuations due to the cubic interaction in the Brazovskii model, using a renormalization scheme motivated by the $1/n$ expansion in the n -vector model in critical phenomena. The fluctuations due to the cubic term have not been addressed in any of the previous studies [18, 42, 43, 44] on block-copolymer systems. We find that in the leading-order approximation these fluctuations stabilize both the BCC phase and the glassy state, thus enlarge the regions of glassy state and ordered state in the phase diagram.

II. MODEL AND SOLUTION

A. Model description

We consider the melt of A-B diblock copolymers of degree of polymerization $N = N_A + N_B$ and block composition $f = N_A/N$. The monomer volume v and Kuhn length b are taken to be the same for both monomers. We describe the thermodynamics of the system using the random-field-approximated (RPA) free-energy functional with local approximations for the cubic and quartic interactions [18, 19, 45] as the Hamiltonian

$$\beta\mathcal{H}[\phi] = \frac{1}{Nv} \left[\frac{1}{2} \int \frac{d^3q}{(2\pi)^3} \phi(-q)\gamma_2(q, -q)\phi(q) + \frac{\gamma_3}{3!} \int d^3x \phi(x)^3 + \frac{\gamma_4}{4!} \int d^3x \phi(x)^4 \right], \quad (1)$$

where $\beta = 1/k_B T$ and the order parameter $\phi \equiv \rho_A(x)v - f$ is the density deviation from the mean value. To simplify the notation, we use the plain x and q to denote the position vector and the wave vector. We also use q to denote the magnitude of the wave vector (the wave number); the context should clarify the difference.

Near the mean-field spinodal $\gamma_2(q, -q)$ can be approx-

imated as

$$\gamma_2(q, -q) = \frac{c^2}{4} (q^2 N b^2 - q_m^2 N b^2)^2 + 2(\chi N)_S - 2\chi N,$$

where χN is the Flory-Huggins interaction parameter between the two blocks, $(\chi N)_S$ is its value at the spinodal, and c is a parameter independent of N . $(\chi N)_S$, c , and q_m are functions of f and N , which can be calculated using the RPA theory of Leibler [19]. Note that, Eq. (1) as a Hamiltonian is applicable to a broad class of copolymer systems, including multiblock copolymers [42] and copolymer/homopolymer blends [46], where the dependence on chain architectures, block compositions, or volume fractions of copolymers can be incorporated in the parameters $(\chi N)_S$, q_m , *etc.* Therefore our results on diblock-copolymer systems should be qualitatively applicable to these systems as well.

The degree of polymerization N plays the role of Ginzburg parameter, which controls the magnitude of fluctuations [18]. To highlight this feature, we nondimensionalize the lengths and wave vectors by the ideal end-to-end distance of the polymer as $\bar{x} \equiv x/(\sqrt{N}b)$, $\bar{q} \equiv q\sqrt{N}b$, $\bar{q}_m \equiv q_m\sqrt{N}b$, and concurrently rescale the order parameter as $\bar{\phi}(\bar{x}) \equiv \phi(x)c\bar{q}_m$, $\bar{\phi}(\bar{q}) \equiv \phi(q)c\bar{q}_m/(\sqrt{N}b)^3$. The Hamiltonian [Eq. (1)] now becomes

$$\begin{aligned} \beta\mathcal{H}[\phi] &= \frac{\sqrt{N}b^3}{v} \left[\frac{1}{2} \int \frac{d^3\bar{q}}{(2\pi)^3} g(q)^{-1} \bar{\phi}(\bar{q})\bar{\phi}(-\bar{q}) + \frac{\eta}{3!} \int d^3\bar{x} \bar{\phi}(\bar{x})^3 + \frac{\lambda}{4!} \int d^3\bar{x} \bar{\phi}(\bar{x})^4 \right] \\ &= \bar{N}^{1/2} H[\bar{\phi}], \end{aligned} \quad (2)$$

where

$$g(q)^{-1} = \frac{1}{4\bar{q}_m^2} (\bar{q}^2 - \bar{q}_m^2)^2 + \tau_0 \bar{q}_m^2, \quad (4)$$

$$\tau_0 = \frac{2(\chi N)_S - 2\chi N}{c^2 \bar{q}_m^4}, \quad (5)$$

$$\eta = \frac{\gamma_3}{c^3 \bar{q}_m^3}, \quad (6)$$

$$\lambda = \frac{\gamma_4}{c^4 \bar{q}_m^4}. \quad (7)$$

The scaled couplings η and λ are respectively the same as $N\Gamma_3$ and $N\Gamma_4$ as defined in Ref. [18]. For notational simplicity, we drop the bars on the variables and the order parameter henceforth.

We point out that, although the parameters in Eq. (1) are written in molecular terms, the model is best interpreted as phenomenological. The random-phase approximation used in deriving Eq. (1), the approximation of higher-order interactions as spatially local [47], and the truncation at quartic order in the order-parameter expansion, all introduce inaccuracies whose effects are difficult to evaluate. Nevertheless, judging from the great success

of the Fredrickson-Helfand theory [which uses the same Hamiltonian as Eq. (1)] in capturing many key features of the physics of diblock-copolymer melts at length scales comparable to or above the size of the polymer chain, we expect that most of our predictions should be qualitatively correct.

In addition, studying glass transitions in the system described by the Hamiltonian [Eq. (1)] is of intrinsic theoretical value, as Eq. (1) corresponds to the weak-coupling limit of the Brazovskii model. Thus our results elucidate the physical behavior of systems in the Brazovskii class in this limit.

The parameter $\bar{N}^{1/2} \equiv N^{1/2}b^3/v$ (henceforth referred to as the ‘‘chain length’’) is a natural combination emerging in any study of the fluctuation effects in polymer melts, which gives the number of other chains within the spatial extension of a single polymer chain [18, 48]. \bar{N} plays a role similar to $1/\hbar$ in quantum field theory [49], *i.e.*, controls the magnitude of fluctuations. In the limit of $\bar{N} \rightarrow \infty$, mean-field behavior is recovered. For systems with large but finite \bar{N} , we can apply a systematic loop expansion using $1/\bar{N}^{1/2}$ as the smallness parameter.

In the next two subsections we outline our perturbative calculation of the order-disorder transition and the glass transition based on such an expansion.

B. Ordered states and order-disorder transition

Our current understanding of the fluctuation effects on the ODT in block-copolymer melts is largely based on the Brazovskii-Leibler-Fredrickson-Helfand (BLFH) theory [18, 19, 40]. This theory uses the self-consistent Brazovskii approximation (a Hartree-type approximation) for the quartic interaction and ignores the fluctuations due to the cubic interaction. Therefore strictly speaking it is only valid for symmetric or nearly symmetric block copolymers. Here we extend this theory to include the leading one-loop correction due to the cubic interaction, which accounts for the fluctuation effects due to asymmetry in the copolymer composition. This improved theory should give more accurate predictions on the ODT

in asymmetric copolymer melts and also enables a consistent comparison with the glass transition in the same system, where cubic term is shown to play a dominant role.

As in previous weak-segregation theories [18, 19], we make the single-mode approximation for the saddle point of the Hamiltonian [Eq. (2)], representing the density wave of the ordered phase by

$$\varphi(x) = a \sum_j [\exp(iQ_j \cdot x) + \exp(-iQ_j \cdot x)], \quad (8)$$

where a is the magnitude of the density wave and Q_j ($1 \leq j \leq n$) are the first set of vectors on the reciprocal lattice of the periodic structure of the ordered microphases [18, 19]. Now we introduce the fluctuation field around the saddle point, $\psi(x) = \phi(x) - \varphi(x)$, and perform an expansion of the Hamiltonian $H[\phi]$ in Eq. (3) around φ . The fluctuation part of $H[\phi]$ is

$$\begin{aligned} \beta\Delta H[\psi; \varphi] &= \beta H[\psi + \varphi] - \beta H[\varphi] \\ &= \frac{1}{2} \int \frac{d^3q}{(2\pi)^3} \psi(-q) g(q)^{-1} \psi(q) + \frac{\eta}{3!} \int d^3x \psi(x)^3 + \frac{\lambda}{4!} \int d^4x \psi(x)^4 \\ &+ \frac{\eta}{2} \int \frac{d^3q_1 d^3q_2 d^3q_3}{(2\pi)^9} \psi(q_1) \psi(q_2) \varphi(q_3) \delta^3(q_1 + q_2 + q_3) \\ &+ \frac{\lambda}{4!} \int \frac{d^3p_1 d^3p_2 d^3p_3 d^3p_4}{(2\pi)^{12}} [4\psi(p_1) \psi(p_2) \psi(p_3) \varphi(p_4) + 6\varphi(p_1) \varphi(p_2) \psi(p_3) \psi(p_4)] \delta^3(p_1 + p_2 + p_3 + p_4). \end{aligned} \quad (9)$$

The linear term of ψ vanishes because φ is at the saddle point. For the quadratic term we only keep the dominant isotropic part

$$D(q)^{-1} = g(q)^{-1} + n\lambda a^2, \quad (10)$$

which is defined as the shifted bare propagator.

The free energy (effective potential) of the microphase-separated system is given by

$$\begin{aligned} \beta F[\varphi] &= -\log \left\langle \exp \left\{ -\bar{N}^{1/2} \beta H[\phi] \right\} \right\rangle \\ &= \beta F_L[\varphi] - \log \left\langle \exp \left\{ -\bar{N}^{1/2} \beta \Delta H[\psi; \varphi] \right\} \right\rangle. \end{aligned} \quad (11)$$

F_L is the Leibler free energy for the ordered phase [19], and the second term in Eq. (11) contains corrections due to the fluctuation part of the Hamiltonian [Eq. (9)]. In the one-loop approximation we have

$$\beta F[\varphi] = \beta F_L(\varphi) + \frac{1}{2\bar{N}^{1/2}} Tr \log \mathcal{G}_H^{-1} - \frac{\lambda}{8\bar{N}} \left[\int \frac{d^3q}{(2\pi)^3} \mathcal{G}_H(q) \right]^2 - \frac{\eta^2}{12\bar{N}} \int \frac{d^3p d^3q}{(2\pi)^6} \mathcal{G}_H(p) \mathcal{G}_H(q) \mathcal{G}_H(-q-p), \quad (12)$$

where $\mathcal{G}_H(q)$ is the Hartree-renormalized propagator determined from

$$\mathcal{G}_H(q)^{-1} = D(q)^{-1} + \frac{\lambda}{2\bar{N}^{1/2}} \int \frac{d^3k}{(2\pi)^3} \mathcal{G}_H(k). \quad (13)$$

Our one-loop approximation is slightly different from the conventional diagrammatic expansion; details are given in Appendix B.

Under this approximation the renormalized correlation function is given by

$$\begin{aligned} \mathcal{G}(q)^{-1} &= \left\{ \frac{\delta^2 \beta F[\varphi]}{\delta \varphi(q) \delta \varphi(-q)} \right\}^{-1} \\ &= \mathcal{G}_H(q)^{-1} - \frac{\eta^2}{2\bar{N}^{1/2}} \int \frac{d^3 k}{(2\pi)^3} \mathcal{G}_H(k) \mathcal{G}_H(q-k). \end{aligned} \quad (14)$$

In the replica calculation $\mathcal{G}(q)$ gives the renormalized diagonal correlation function in the replica space.

C. Random structures and glass transition

Traditionally two different approaches have been developed to study frustrated systems with quenched disorder. The dynamic approach, most notably the mode-coupling theory [50], focuses on the dynamic correlation function (*e.g.*, the Edwards-Anderson order parameter defined as the long-time correlation function of the spins in the Ising-spin-glass model [51]) and thus characterizes the glassy state with nonvanishing long-time correlation or broken ergodicity. On the other hand, the thermodynamic or equilibrium approach, including the density

functional approach [52] and the replica approach [53], describes glass transitions in terms of the energy landscape. The connection between these two approaches was first demonstrated in the mean-field-spin-glass models [53, 54]. Recently Monasson [31] proposed a thermodynamic approach to studying metastable states in structural glasses resulting from self-generated randomness. This equilibrium approach captures the dynamic feature of the glass transition as well as the thermodynamics, and has successfully predicted the glass transitions in the Coulomb-frustrated-magnet model [36]. Here we use this thermodynamic approach to study the random structures in block-copolymer melts.

The central idea is to introduce an external pinning field ζ and calculate the free energy of the system pinned by ζ

$$F[\zeta] = -k_B T \log Z[\zeta] = -k_B T \log \int \mathcal{D}\phi \exp \left(-\frac{1}{k_B T} \left\{ \mathcal{H}[\phi] + \frac{\alpha}{2} \int d^3 x [\phi(x) - \zeta(x)]^2 \right\} \right), \quad (15)$$

where $\alpha > 0$ is the coupling between the pinning field and the order parameter. The effect of ζ is to localize the system into the basins of energy minima; one easily sees that the minima of the free energy $F[\zeta]$ coincide with those of $\mathcal{H}[\phi]$. The field ζ serves as a running index for labeling different basins on the energy landscape, and sampling the configuration space of ζ thus provides information on the metastable free-energy minima (the energy minima with their local fluctuations) of the unperturbed system governed by \mathcal{H} . Therefore one can use $F[\zeta]$ as an “effective Hamiltonian” for the metastable free-energy minima and compute the “quenched-average” free energy

$$\bar{F} = \frac{\int \mathcal{D}\zeta F[\zeta] \exp \{-F[\zeta]/k_B T\}}{\int \mathcal{D}\zeta \exp \{-F[\zeta]/k_B T\}}. \quad (16)$$

If the system is fully ergodic, as $\alpha \rightarrow 0^+$, \bar{F} should be equal to the equilibrium free energy $F = -k_B T \log \int \mathcal{D}\phi \exp\{-\mathcal{H}[\phi]/k_B T\}$ in the thermodynamic limit. However, when ergodicity is broken $\lim_{\alpha \rightarrow 0^+} \bar{F}$ can be different from F . Their difference

$$\delta F = \bar{F} - F = T S_c, \quad (17)$$

gives the configurational entropy which is lost due to the trapping at local metastable free-energy minima. S_c defined above is a measure of the configurational complexity due to an exponentially large number of metastable free-energy minima [31, 36, 53].

To calculate S_c it is convenient to introduce the “replicated” free energy

$$F_m = - \lim_{\alpha \rightarrow 0^+} \frac{k_B T}{m} \log \int \mathcal{D}\zeta \exp \left\{ -\frac{m}{k_B T} F[\zeta] \right\} = - \lim_{\alpha \rightarrow 0^+} \frac{k_B T}{m} \log \int \mathcal{D}\zeta Z[\zeta]^m = -\frac{k_B T}{m} \log Z_m, \quad (18)$$

where T/m is introduced as the effective temperature conjugate to the “effective Hamiltonian” $F[\zeta]$. \bar{F} and S_c are

obtained from Eq. (18) straightforwardly as

$$\bar{F} = \left. \frac{\partial(mF_m)}{\partial m} \right|_{m=1}, \quad (19)$$

$$S_c = - \left. \frac{\partial F_m}{\partial(T/m)} \right|_{m=1} = \frac{1}{T} \left. \frac{\partial F_m}{\partial m} \right|_{m=1}. \quad (20)$$

When m is an integer, Z_m in Eq. (18) can be simplified by introducing m copies of ϕ and integrating out the ζ field, which gives

$$Z_m = \lim_{\alpha \rightarrow 0^+} \int \mathcal{D}\phi_a \exp \left\{ -\frac{1}{k_B T} \sum_{a=1}^m \mathcal{H}[\phi_a] - \frac{\alpha}{2mk_B T} \sum_{1 \leq a < b \leq m} \int d^3x [\phi_a(x) - \phi_b(x)]^2 \right\}. \quad (21)$$

Eq. (21) has the same form as the replicated partition function for a random system with quenched disorder [53], although here we are interested in the physical limit corresponding to $m = 1$. To characterize the physical states of the system, we introduce the (renormalized) correlation functions $\mathcal{G}(q) = \langle \phi_a(q)\phi_a(-q) \rangle$ and $\mathcal{F}(q) = \langle \phi_a(q)\phi_b(-q) \rangle_{a \neq b}$. $\mathcal{G}(q)$ is the normal physical correlation function of the system, whereas $\mathcal{F}(q)$ measures the correlation between different replicas. At high temperatures the system is ergodic, and in the limit $\alpha \rightarrow 0^+$ different replicas are uncoupled. Thus $\mathcal{F}(q) = 0$. When ergodicity is spontaneously broken, different replicas become coupled even in the limit $\alpha \rightarrow 0^+$, and $\mathcal{F}(q) \neq 0$. Note that the correlation function $\mathcal{F}(q)$ can be interpreted as the correlation of the same system separated by a long time span, which is essentially an Edwards-Anderson order parameter. Using $\mathcal{F}(q)$ as the order parameter for ergodicity breaking, we can define the onset of glassiness T_A as the temperature when there first appears a solution with $\mathcal{F}(q) \neq 0$. T_A defined in this way coincides with the dynamic-transition temperature in mean-field-spin-glass models characterized by the appearance of drastically slowed dynamic relaxation [31, 36].

To obtain the replica free energy defined by Eq. (18), we adopt the self-energy approach [49] and express the effective potential F_m as a functional of \mathcal{G} and \mathcal{F}

$$\beta F_m[\mathbf{G}] = \frac{1}{m} \left\{ \frac{1}{2} \text{Tr} \log \mathbf{G}^{-1} + \frac{1}{2} \text{Tr} (\mathbf{D}^{-1} \cdot \mathbf{G}) - \Gamma_2[\mathbf{G}] \right\}, \quad (22)$$

with

$$\mathbf{G} = (\mathcal{G} - \mathcal{F}) \mathbf{I} + \mathcal{F} \mathbf{E}, \quad (23)$$

where $E_{ab} = 1$, $I_{ab} = \delta_{ab}$. (Henceforth we use the bold face uppercase letters (\mathbf{G} , \mathbf{D} , $\mathbf{\Sigma}$) for the matrices of functions in the replica space, and use the plain uppercase letters (G , D , *etc.*) when referring to the matrix elements.) G_{ab} is the renormalized correlation function with replica indices a, b . D_{ab} is the replica-symmetric bare correlation function, $D_{ab}(q) = g(q)\delta_{ab}$, with $g(q)$ given from Eq. (4)

$$q_m^{-2} g(q)^{-1} = \frac{1}{4} \left(\frac{q^2}{q_m^2} - 1 \right)^2 + \tau_0.$$

The self-energy functions Σ_{ab} are defined by

$$\mathbf{\Sigma} = \mathbf{G}^{-1} - \mathbf{D}^{-1}, \quad (24)$$

and obtained through minimization of Eq. (22)

$$\mathbf{\Sigma} = - \frac{2\delta\Gamma_2[\mathbf{G}]}{\delta\mathbf{G}}. \quad (25)$$

$\Gamma_2[\mathbf{G}]$ contains all two-particle-irreducible (2PI) diagrams, which is evaluated perturbatively. Detailed calculations are given in Appendix A.

Taking the inverse of the matrix \mathbf{G} defined in Eq. (23), we find the self-energy from Eq. (24) takes the following form

$$\Sigma_{ab} = (\Sigma_{\mathcal{G}} - \Sigma_{\mathcal{F}})\delta_{ab} + \Sigma_{\mathcal{F}}, \quad (26)$$

where

$$\Sigma_{\mathcal{G}}(q) = \mathcal{G}(q)^{-1} - g(q)^{-1}, \quad (27)$$

$$\Sigma_{\mathcal{F}}(q) = \mathcal{G}(q)^{-1} - \frac{1}{\mathcal{G}(q) - \mathcal{F}(q)}. \quad (28)$$

Assuming the momentum dependence of self-energy functions $\Sigma_{\mathcal{G}}(q)$ and $\Sigma_{\mathcal{F}}(q)$ to be negligible compared with $g(q)$, we can approximate the renormalized diagonal correlation function as

$$q_m^{-2}\mathcal{G}(q)^{-1} \approx \frac{1}{4} \left(\frac{q^2}{q_m^2} - 1 \right)^2 + \tau_0 + \Sigma_{\mathcal{G}}(q_m)q_m^{-2} \equiv \frac{1}{4} \left(\frac{q^2}{q_m^2} - 1 \right)^2 + r. \quad (29)$$

And the off-diagonal correlation function $\mathcal{F}(q)$ takes the form

$$\mathcal{F}(q) = \mathcal{G}(q) - \frac{1}{\mathcal{G}(q)^{-1} - \Sigma_{\mathcal{F}}(q)} \quad (30)$$

$$\approx \frac{q_m^{-2}}{\frac{1}{4} \left(\frac{q^2}{q_m^2} - 1 \right)^2 + r} - \frac{q_m^{-2}}{\frac{1}{4} \left(\frac{q^2}{q_m^2} - 1 \right)^2 + r - q_m^{-2}\Sigma_{\mathcal{F}}(q_m)} \quad (31)$$

$$\equiv \frac{q_m^{-2}}{\frac{1}{4} \left(\frac{q^2}{q_m^2} - 1 \right)^2 + r} - \frac{q_m^{-2}}{\frac{1}{4} \left(\frac{q^2}{q_m^2} - 1 \right)^2 + s}. \quad (32)$$

Eqs. (24) and (25) give the self-consistent equations for \mathcal{G} and \mathcal{F} (in our case algebraic equations for r and s .) Solving these equations we obtain a normal replica-symmetric solution with $r = s$ and a replica-symmetry-broken solution with $r < s$ below the dynamic-transition temperature T_A (corresponding to some $(\chi N)_A$ in our diblock-copolymer model.)

The configurational entropy is obtained from Eqs. (20) and (22) to be

$$\frac{S_c}{k_B} = -\frac{1}{2} \int \frac{d^3q}{(2\pi)^3} \left[\log \left(1 - \frac{\mathcal{F}(q)}{\mathcal{G}(q)} \right) - \frac{\mathcal{F}(q)}{\mathcal{G}(q)} \right] - \frac{\partial}{\partial m} \left(\frac{\Gamma_2}{m} \right) \Big|_{m=1}. \quad (33)$$

One indeed finds that S_c becomes extensive below T_A and decreases as the temperature drops further. At $T = T_K$, S_c vanishes and the system becomes completely frozen. This temperature is identical to the so-called Kauzmann temperature [55], which is the limit of supercooling below which the system gets vitrified inevitably. Physically this means that a finite number of free-energy minima dominate over the other metastable states; therefore the quenched-average free energy is again equal to the thermodynamic average.

III. RESULTS AND DISCUSSION

A. Glass transition

Glass transitions in the Coulomb-frustrated-magnet model have been addressed by several groups in recent years [35, 36, 37, 41, 56, 57, 58, 59]. These studies establish that glass transitions are always possible and could be kinetically favored. However, all these studies focus on the strong-coupling regime, and except for Ref. [37] the asymmetric cubic interaction has been ignored. The block-copolymer system we are studying belongs to the same universality class as the Coulomb frustrated magnet – both are examples of the Brazovskii model. But for long polymers our system corresponds to the weak-coupling regime of the Brazovskii model. Furthermore, the presence of the cubic interaction, which reflects compositional asymmetry in the copolymer, is the rule rather than exception. It has a strong effect on the ODT and

the glass transition, as we will discuss in this work.

We start with the glass transition. Figure 1 shows the transition lines for two different chain lengths, $\bar{N} = 10^4$ and $\bar{N} = 5 \times 10^4$. The dash-dotted lines represent the onset of glassiness (or the dynamic-glass-transition temperature [36]) T_A , and the dashed lines represent the Kauzmann temperature (or the thermodynamic-glass-transition temperature [36]) T_K . The interpretations of these two transitions are the same as in the energy-landscape theory of glass transitions: T_A signals the onset of glassy behavior (*e.g.*, slow relaxations) in the supercooled state, whereas T_K represents the limit of supercooling below which the system becomes vitrified [38]. (Note that we use the term “temperature” even though the phase diagram is presented in terms of the Flory-Huggins interaction parameter χN ; the actual temperature can be determined from the temperature dependence of χN .) These results show that for diblock-copolymer melts, glass transitions occur at finite temperatures at any chain composition f . Furthermore, as the chain length increases, both T_A - and T_K -transition lines approach the mean-field spinodal. This latter result is consistent with our anticipation that a large number of inhomogeneous metastable free-energy minima emerge as the system approaches the mean-field spinodal.

Figure 1 also shows the full crossover from nearly symmetric copolymer, whose glass transitions are dominated by the quartic coupling, to highly asymmetric copolymer dominated by the cubic coupling. For symmetric or nearly symmetric copolymer, it is well known [18, 60] that the mean-field spinodal is destroyed by the fluc-

tuations and the disordered phase is always locally stable. And the transition from the disordered phase to the LAM phase is a first-order transition with rather complicated (and probably slow) kinetics [61]. Therefore a deep quench without annealing can result in the trapping of the system in randomly microphase-separated structures; these are the glassy structures captured in our work. This scenario is consistent with the experimental observations of Bates *et al.* [8], where they studied the mechanical properties of three different samples: a rapidly quenched sample, a slowly supercooled sample, and a shear-oriented sample. By analogy to molecular liquids, these three samples can be likened to the glassy state, the supercooled-liquid state, and the ordered crystalline state respectively. The quenched sample in this study exhibits solidlike responses at low frequencies while the supercooled sample has typical liquidlike responses. In addition, the dynamic moduli of the quenched sample are higher than those of the ordered sample; this behavior is consistent with the finding that in bulk-metallic-glassy state is generally stronger and tougher than the crystalline counterpart [62].

We notice that in going from symmetric to asymmetric compositions on either side, the transition lines exhibit a minimum. This is attributed to the crossover from the quartic-coupling dominant regime to the cubic-coupling dominant regime. As we discuss later, the cubic term considerably stabilizes the glassy state and enlarges the region of glassy state in the phase diagram. This results in the initial drop of χN values at the transitions as f deviates from 0.5.

For very asymmetric copolymers, mean-field theory predicts a first-order transition into ordered spherical phases [face-centered cubic (FCC) or BCC] at χN smaller

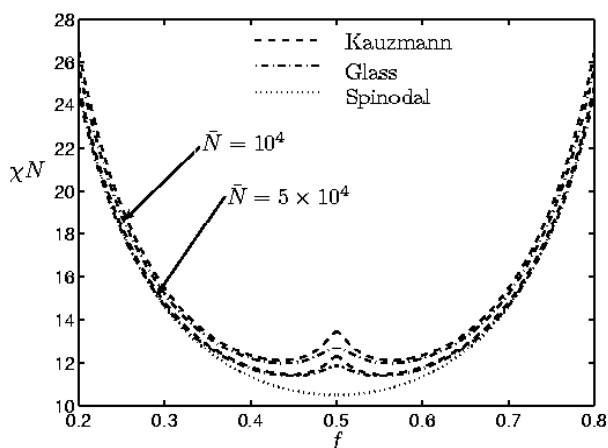


FIG. 1: Glass transitions in diblock-copolymer melt. Dashed lines for the Kauzmann temperature; dash-dotted lines for the onset of glassiness; dotted line for the mean-field spinodal. The upper dashed and dash-dotted lines for chain length $\bar{N} = 10^4$; the lower ones for $\bar{N} = 5 \times 10^4$.

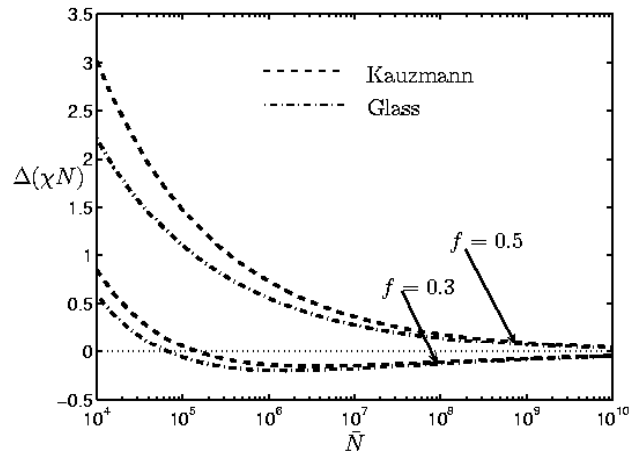


FIG. 2: Chain-length dependence of glass transitions. Plot of $\Delta(\chi N) \equiv \chi N - (\chi N)_S$ against \bar{N} . Dashed lines for the Kauzmann temperature; dash-dotted lines for the onset of glassiness. Upper dashed and dash-dotted lines for the symmetric copolymer; lower lines for the asymmetric copolymer with $f = 0.3$.

than the mean-field spinodal $(\chi N)_S$ [12]. However, experiments show that between the featureless disordered phase and the ordered BCC phase, there exists an intervening disordered-micelle state (which, by the way, excludes the FCC phase from being the most stable state [29, 30].) These disordered micelles are most likely the structural entities responsible for the formation of the glassy state. In a self-consistent-field calculation, it was shown that [30] the micelles are formed via a thermally activated process, with a free-energy barrier that vanishes at the mean-field spinodal. Therefore, if the system is quickly quenched to the vicinity of the spinodal, micelles will appear in large numbers all over the sample. The jamming of these micelles causes their translational diffusion to be so slow that long-range periodic order can not develop. The interplay between the glass transition and the ODT is complicated. We will present some tentative discussions in the next subsection. But here we simply note that, in contrast to the symmetric case where glass transitions occur at $\chi N > (\chi N)_S$ (or below the mean-field spinodal temperature), for asymmetric copolymer glass transition can occur at $\chi N < (\chi N)_S$ (or above the mean-field spinodal temperature.) We attribute this to the fact that the different arrangements of micelles could generate a large number of metastable states, which stabilize the glassy state.

As highlighted in Eq. (3), the chain length \bar{N} controls the importance of nonlinear fluctuation effects, and hence the deviation from mean-field behavior that is recovered in the limit $\bar{N} \rightarrow \infty$. Figure 2 shows the chain-length dependence of the glass transition temperatures [measured by $(\chi N)_A$ and $(\chi N)_K$ respectively] relative to the mean-field spinodal for the symmetric copolymer and the

asymmetric one with $f = 0.3$. It is clear that in both cases the glass transitions (both T_A and T_K) approach the mean-field spinodal as \bar{N} goes to infinity (though from different directions in the symmetric and asymmetric cases), implying that in the limit of long chains the mean-field spinodal is the true stability limit of the disordered phase (with respect to either ordered or randomly phase-separated structures.) In other words, the mean-field spinodal is ultimately responsible for the appearance of random structures, thus is the mean-field signature for the glass transition. This general conclusion is likely to be universal to the class of models with continuous degeneracy in the ground states, such as the Brazovskii model (see Ref. [59] for other models of the same class.)

We now discuss the chain-length dependence of the gap between glass transitions and the spinodal, $(\chi N)_A - (\chi N)_S$ and $(\chi N)_K - (\chi N)_S$. By a simple scaling analysis given in Appendix C, we find that both scale as $\bar{N}^{-0.3}$ for symmetric composition. This is consistent with the analysis of Wolynes *et al.* [37] if we substitute the \bar{N} dependence of the parameters into their scaling relation. Our more accurate numerical calculations confirm this result, as shown in Fig. 3, where the first-order transition temperature into LAM phase is also included for comparison. For asymmetric copolymers, the results are more complicated: for short chains, both $(\chi N)_A$ and $(\chi N)_K$ are larger than the spinodal value $(\chi N)_S$; as \bar{N} increases, the transition lines are first shifted downward below the spinodal line, which indicates a possible crossover; then for even larger \bar{N} , the transitions gradually approach the spinodal, and eventually collapse to the spinodal as $\bar{N} \rightarrow \infty$. In this latter limit, we find, using the scaling analysis outlined in Appendix C, that $(\chi N)_S - (\chi N)_{A,K} \sim \bar{N}^{-1/4}$. The nonmonotonic dependence on \bar{N} is due to the presence of the cubic term. Figure 2 also suggests a crossover from the quartic-coupling dominant to the cubic-coupling dominant regime as chain length increases. At a given f , quartic coupling dominates for short chains and the glass-transition lines are located above the spinodal (or below the spinodal temperature); for long chains the opposite holds.

We close this subsection with a brief discussion of the dynamics of the system. For the Coulomb-frustrated-magnet model, by invoking the entropy-droplet picture, Wolynes *et al.* predicted [36, 63] that the system should exhibit relaxations similar to fragile liquids [64], characterized by the Vogel-Fulcher behavior, with a relaxation time $\tau \propto \exp[A/(T - T_K)]$ between T_A and T_K , and diverging at the Kauzmann temperature T_K . This prediction was disputed by Geissler and Reichman [58], who performed dynamic-Monte-Carlo simulations of the Brazovskii model without the cubic interaction. They found that as the system approaches the glass-transition temperature predicted by the mode-coupling theory, the relaxation time indeed increases dramatically, but does not show characteristics of fragile liquids. Schmalian *et al.* subsequently argued [65] that the failure to find the expected dynamic behavior could be a result of the partic-

ular approximations used in the mode-coupling approximation which overestimates the transition temperature. Furthermore, the simulations were performed for temperatures above the ODT temperature. But our calculations show that in the absence of the cubic interaction, the onset of glassiness always occurs below the ODT temperature, at least in the weak-coupling regime. Thus the dynamic behavior of these systems remain an unresolved issue.

For block-copolymer melts, the situation is even more complicated. The Hamiltonian given by Eq. (1) is a coarse-grained description of the system that focuses on the physics at length scales comparable to or larger than the size of the polymer. Therefore we expect the validity of our analysis to be limited to this range of length scales. The configurational entropy S_c defined above only measures the number of configurations of chain aggregates in the locally phase-separated structures, but does not account for the different chain conformations within each aggregate. Indeed, above the glass transition temperature of the *monomer*, the polymer chains remain liquidlike even though the system acquires solidlike behavior at the microstructural scale. Chain diffusion provides an additional mechanism for relaxations. Therefore, to accurately describe the dynamic relaxations in block-copolymer melts, one has to consider relaxations both at the microstructural scale and of individual chains.

B. Glass transition vs. order-disorder transition

Our results in the previous subsection show that the glass transition is possible in diblock-copolymer melts, and it is related to the underlying mean-field spinodal of the disordered phase, which is responsible for the proliferation of inhomogeneous metastable states. However, the ODT also occurs in the neighbourhood of the spinodal. Thus a full understanding of the glass transition in this system must address the relationship between these two transitions.

In molecular liquids the glass transition always takes place in the supercooled liquid state, *i.e.*, below the melting (freezing) temperature. However, in diblock-copolymer melts, the structural entities forming the random structures are themselves molecular aggregates formed through self-assembly, the number and size of which depend on the temperature of the system. Therefore the relationship between the glass transition and the ODT is not obvious at all.

Microphase transitions in block-copolymer systems have been extensively studied, both theoretically and experimentally [1, 3]. However, existing theoretical treatments of asymmetric copolymers ignore the fluctuations due to the cubic interaction in the Hamiltonian. Our analysis in the previous subsection shows that these fluctuations have strong stabilizing effects on the glassy state in asymmetric diblock copolymers, at least for long chains. (In the system of short chains the situation is

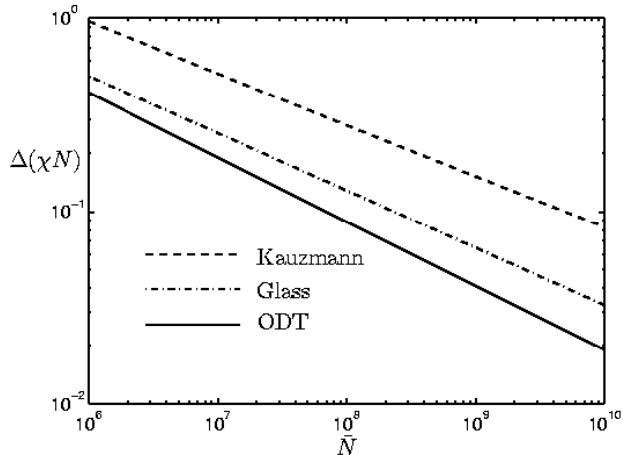


FIG. 3: Glass transition vs. ODT in symmetric copolymer melts. Dashed and dash-dotted lines have the same meanings as in Fig. 2; the solid line represents the ODT into LAM phase.

ambiguous as the higher-order diagrammatic terms neglected in our analysis could become important.) We thus expect that the cubic term can have similar important effects on the ODT [67]. In this subsection, we compare the phase boundaries of the ordered phase and of the glassy state. We choose to study the symmetric copolymer ($f = 0.5$) and the highly asymmetric copolymer $f \sim 0.1$, as our perturbative methods are better controlled in these two limits (dominated by the quartic and cubic nonlinear interactions respectively.)

Figure 3 shows the values of χN with reference to the spinodal $(\chi N)_S$, as a function of the chain length \bar{N} , for the ODT into LAM phase and the glass transitions in symmetric copolymers. The solid line represents the ODT and the dashed and the dash-dotted lines represent the glass transitions. The ODT is calculated using a one-loop approximation in the self-energy, similar to the self-consistent Brazovskii approximation used by Fredrickson and Helfand [18]. We observe the scaling of $(\chi N)_{ODT} - (\chi N)_S \sim \bar{N}^{-1/3}$ as predicted in Ref. [18]. For the onset of glassiness, $(\chi N)_A - (\chi N)_S$ scales as $\bar{N}^{-0.3}$, which agrees well with our approximate scaling analysis given in Appendix C. For the Kauzmann temperature, the numerical solution gives a scaling of $\sim \bar{N}^{-0.27}$, which is slightly less than the approximate scaling prediction $\sim \bar{N}^{-0.3}$. Our results show that for symmetric copolymers, the ODT always occurs before the glass transitions (*i.e.*, at temperatures above the glass transitions.) While one might argue that this conclusion could be a result of the particular choice of diagrams included in our perturbative calculation, we find that this scaling with \bar{N} remains unchanged when a different approximation scheme, the self-consistent-screening approximation, is used [68]. In addition, our results are also consistent with the local-field calculations by Wu *et al.* [37],

as will be discussed below. Since $(\chi N)_{ODT} - (\chi N)_S$ decays more rapidly with \bar{N} than both $(\chi N)_A - (\chi N)_S$ and $(\chi N)_K - (\chi N)_S$, for sufficiently large \bar{N} , we always have $(\chi N)_{ODT} < (\chi N)_{A,K}$. Therefore, at least in the long-chain limit, our conclusion that the glass transition occurs below the ODT temperature should be valid, regardless of the approximations in the calculation. This result implies that the random structures are obtained as a result of supercooling past the LAM ordering temperature, and are thus metastable with respect to the ordered LAM phase. This is consistent with the experimental observation [8] that annealing the isotropic supercooled sample leads to better ordered LAM structure, suggesting that LAM phase is the equilibrium state with lowest free energy.

Figure 4 shows the various transitions for highly asymmetric copolymers around $f = 0.1$. In the case of $\bar{N} = 10^7$, the glass transition lines are located below the ODT, *i.e.*, the glass transition temperatures are above the ODT temperature. In other words, glass transitions can precede the ordering transition into BCC phase; the glassy state can be thermodynamically stable while both the disordered and the ordered phases are metastable. This unusual behavior is quite different from what appears in molecular fluids, where the glass transition always occurs below the melting (ordering) temperature. For the longer chain of $\bar{N} = 10^8$, the ODT occurs before the glass transitions; this is the expected behavior in the asymptotic limit of long chains, since in this limit the glass transition lines approach the mean-field spinodal whereas the ODT into BCC phase takes place at a finite distance below the spinodal [12].

The chain-length dependence of the glass transitions relative to the ODT for asymmetric diblock copolymers is qualitatively similar to the critical micelle temperature in the same system. There it is shown that [30] the disordered micelles can appear in large numbers before the ordering transition only for chains that are not too long; for very long polymers, ODT will set in before the disordered micelles reach a considerable concentration, essentially precluding the disordered micelles from being a distinct intervening phase between the featureless disordered state and the ordered spherical (FCC or BCC) phases. Since micelles are likely to be the structural entities in the glassy state, the connection between the micelle formation and the glass transition in asymmetric diblock-copolymer melts is worth further investigating.

As alluded to in Sec. III A, the cubic interaction stabilizes the glassy state. We attribute this stabilizing effect to the additional complexities in the configurational space caused by the cubic term. This effect is closely related to the effect of the cubic interaction on the ODT. Theoretical analysis shows that the presence of the cubic term can considerably reduce the free energy of ordered microstructures with three fold symmetries. This is consistent with the fact that there are more stable ordered phases in asymmetric diblock copolymers. If we visualize the random structures as polycrystals with local but no

long-range order, then the increased variety of mesophase structures will increase the complexity in the configuration space [69], which can explain the stabilization of the glassy state in asymmetric copolymers.

As a final technical point, we compare our treatment of the cubic term with that in Ref. [37]. There the authors used a local-field approximation, in which a momentum independent self-energy is solved variationally by mapping the Brazovskii Hamiltonian [as given by Eq. (2)]

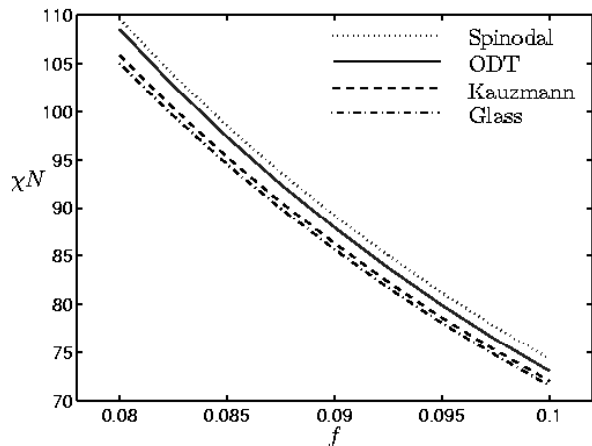
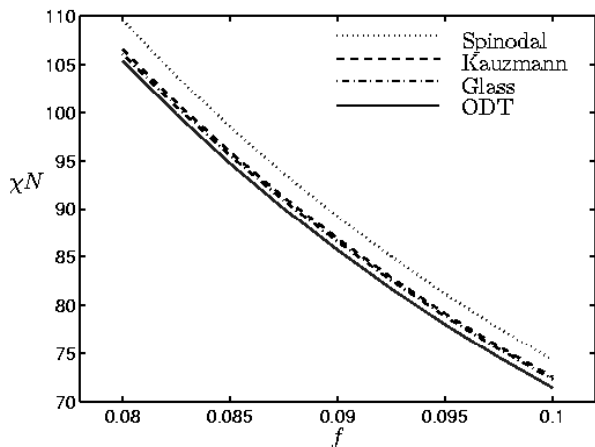
(a) $\bar{N} = 10^7$ (b) $\bar{N} = 10^8$

FIG. 4: Glass transition vs. ODT in very asymmetric copolymer. (a) $\bar{N} = 10^7$, from above: mean-field spinodal (dotted line), ODT (solid line); Kauzmann temperature (dashed line); onset of glassiness (dash-dotted line.) (b) $\bar{N} = 10^8$, from above: mean-field spinodal (dotted line), Kauzmann temperature (dashed line), onset of glassiness (dash-dotted line), ODT (solid line.)

to a reference nonlinear but local Hamiltonian. Within this approximation, it was found that the cubic interaction considerably stabilizes the glassy state and the glass transition can occur at temperatures above the mean-field spinodal temperature; these results coincide with ours. However, for certain choices of parameters in the weak-coupling regime, this local-field treatment could result in a nonmonotonic relation between the correlation length and the temperature. We believe this unphysical behavior is probably due to overestimating the fluctuation effects due to the cubic term in their treatment.

IV. CONCLUSIONS

To conclude, using the thermodynamic replica formalism we have shown that at low temperatures, diblock-copolymer melts can exist as randomly microphase-separated structures, in addition to the thermodynamically stable periodic structures. This transition is essentially a glass transition in which the supercooled liquid gradually gets vitrified. We have identified the temperature range over which this glass transition can occur, which is bordered by the onset of glassiness (or the dynamic glass transition) temperature from above and the Kauzmann (thermodynamic glass transition) temperature from below. For symmetric diblock copolymers, the glass transition takes place below the ODT temperature into LAM phase. However, for asymmetric diblock copolymers, the glass transition can precede the ordering transition, which is an unusual feature that probably reflects the self-assembly nature of the system. This study leads us to naturally identify the quenched samples of block copolymers in some previous experimental works as the glassy state of the system. Given the slow phase separation kinetics in copolymer melts, we expect such glassy structures to be quite common in systems without externally imposed aligning fields.

Like in any fluctuation theories on polymer mixtures [18, 48], the scaled degree of polymerization \bar{N} serves as a Ginzburg parameter which allows us to systematically examine the approach to mean-field behavior as $\bar{N} \rightarrow \infty$. An important conclusion is that in the limit of infinite long chains, the glass transitions collapse to the mean-field spinodal, suggesting that the mean-field spinodal is ultimately responsible for the proliferation of inhomogeneous free-energy minima and can be used as the mean-field signature for the glass transition.

Studying diblock-copolymer melt as a specific example of the Brazovskii model, we find that the cubic interaction significantly increases the stability of the glassy state as well as the BCC phase and causes qualitative changes in the scaling relations with the chain length. We conjecture that this stabilizing effect is due to the increased configurational complexity as a result of more free-energy minima due to the presence of the cubic term.

Acknowledgments

Engineering of Materials at Caltech.

This work was supported by the National Science Foundation through the Center for the Science and En-

APPENDIX A: PERTURBATIVE EXPANSION OF THE EFFECTIVE POTENTIAL WITH REPLICA SYMMETRY BREAKING

In this appendix we present the details of our perturbative calculation of the free energy defined in Eq. (18). The general expansion of the effective potential for a system with symmetry breaking was derived in Ref. [49]. Here we omit the details of the derivation but give the result

$$\Gamma[\varphi, \mathbf{G}] = I[\varphi] + \frac{1}{2}Tr \log \mathbf{G}^{-1} + \frac{1}{2}Tr (\mathbf{D}^{-1} \cdot \mathbf{G}) - \Gamma_2[\mathbf{G}; \Delta H]. \quad (\text{A1})$$

Here φ is the order parameter in the ordered phase; $I[\varphi]$ is the mean-field free energy [in our case the Leibler free energy $F_L(\varphi)$]; $\Delta H[\varphi; \psi]$ is the shifted Hamiltonian [see Eq. (9)]; \mathbf{D} is the shifted bare propagator

$$D_{ab}(q) = \frac{\delta^2 \beta \Delta H[\varphi]}{\delta \varphi_a(q) \delta \varphi_b(-q)}, \quad (\text{A2})$$

and \mathbf{G} is the renormalized propagator. As noted before, we reserve bold-face uppercase letters for matrices of correlation functions and the corresponding plain ones for the matrix elements. The second term ($Tr \log$) in Eq. (A1) is the one-loop correction and the last term Γ_2 includes higher-order corrections, including all 2PI diagrams generated by the vertices in the shifted Hamiltonian ΔH with the renormalized propagator \mathbf{G} . The third term ensures the consistency of the expansion in terms of the renormalized propagator.

It has been shown in Ref. [49] that $\Gamma[\varphi, \mathbf{G}]$ as defined in Eq. (A1) is stationary with respect to both φ and \mathbf{G} . Therefore one can derive the self-energy equations through a variation of Eq. (A1), which gives

$$\frac{\delta \Gamma[\mathbf{G}]}{\delta \mathbf{G}} = 0 \Rightarrow \boldsymbol{\Sigma} = \mathbf{G}^{-1} - \mathbf{D}^{-1} = -\frac{2\delta \Gamma_2[\mathbf{G}]}{\delta \mathbf{G}}. \quad (\text{A3})$$

In the field theory description of diblock-copolymer melts [Eq. (3)], $\bar{N}^{-1/2}$ serves as a smallness parameter, which enables a straightforward loop expansion for $\Gamma_2[\mathbf{G}]$. To the leading two-loop order (one-loop order in the self-energy), one has three terms

$$\Gamma_2^{(1)} = -\frac{\lambda}{8\bar{N}} \sum_a \int \frac{d^3 q_1 d^3 q_2}{(2\pi)^6} G_{aa}(q_1) G_{aa}(q_2), \quad (\text{A4a})$$

$$\Gamma_2^{(2)} = \frac{\eta^2}{12\bar{N}} \sum_{a,b} \int \frac{d^3 q_1 d^3 q_2}{(2\pi)^6} G_{ab}(q_1) G_{ab}(q_2) G_{ab}(-q_1 - q_2), \quad (\text{A4b})$$

$$\Gamma_2^{(3)} = \frac{\lambda^2}{12\bar{N}} \sum_{a,b} \int \frac{d^3 q_1 d^3 q_2 d^3 q_3}{(2\pi)^9} \varphi_a(q_1) G_{ab}(q_2) G_{ab}(q_3) G_{ab}(q_1 + q_2 + q_3) \varphi_b(-q_1), \quad (\text{A4c})$$

corresponding to the diagrams shown in Fig. 5(a), (b), and (c) respectively. In the glassy state, the translational-symmetry-breaking does not occur; therefore $\varphi = 0$, $D_{ab}(q) = g(q)\delta_{ab}$, and $\Gamma_2^{(3)}$ vanishes. Note that $\Gamma_2^{(1)}$ is the Hartree term which only generates a momentum-independent self-energy in the diagonal part of \mathbf{G} and $\Gamma_2^{(2)}$ generates an off-diagonal self-energy which enables a nontrivial solution with broken replica symmetry. For symmetric copolymer, the cubic coupling vanishes. Therefore to study the possibility of broken replica symmetry we need to include the next order off-diagonal term

$$\Gamma_2^{(4)} = \frac{\lambda^2}{48\bar{N}^{3/2}} \sum_{a,b} \int \frac{d^3 q_1 d^3 q_2 d^3 q_3}{(2\pi)^9} G_{ab}(q_1) G_{ab}(q_2) G_{ab}(q_3) G_{ab}(-q_1 - q_2 - q_3), \quad (\text{A4d})$$

corresponding to the three loop diagram as shown in Fig. 5(d). To study the crossover from very asymmetric to symmetric copolymer, we keep $\Gamma_2^{(4)}$ in the off-diagonal renormalization for asymmetric copolymer as well. From

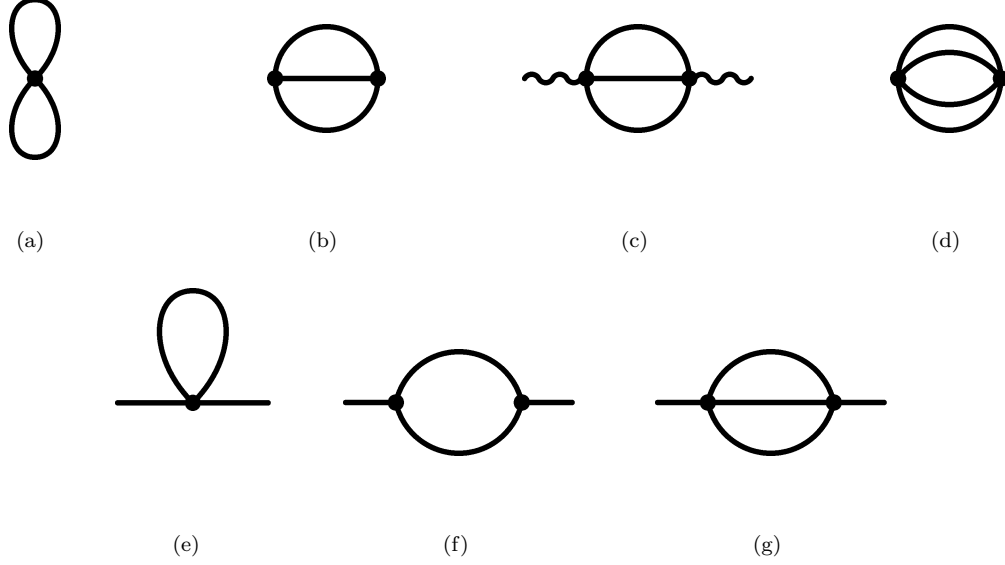


FIG. 5: Feynman diagrams: (a)-(d) Loop diagrams in Γ_2 ; (e)-(g) Self-energy diagrams. In the diagrams thick solid lines represent the renormalized propagator \mathbf{G} and wiggly lines represent the external leg of the order parameter $\varphi(q)$. We use a slightly different perturbative expansion for the diagonal renormalization, as explained in Appendix B.

Eqs. (A3) and (A4) we obtain the self-energy

$$\Sigma_{ab}(k) = \frac{\lambda}{2N^{1/2}} \int \frac{d^3q}{(2\pi)^3} G_{aa}(q) \delta_{ab} - \frac{\eta^2}{2N^{1/2}} \int \frac{d^3q}{(2\pi)^3} G_{ab}(q) G_{(ab)}(k-q) - \frac{\lambda^2}{6N} \int \frac{d^3q d^3p}{(2\pi)^6} G_{ab}(q) G_{ab}(p) G_{ab}(k-p-q). \quad (\text{A5})$$

The three terms on the right hand side corresponding to Fig. 5(e), (f), and (g) respectively.

Under the one-step-replica-symmetry-breaking (1-RSB) ansatz, $G_{ab}(q) = [\mathcal{G}(q) - \mathcal{F}(q)] \delta_{ab} + \mathcal{F}(q)$, and Γ_2 has three terms from Eqs. (A4a), (A4b), and (A4d)

$$\Gamma_2^{(1)} = -\frac{m\lambda}{8N} \left(\int \frac{d^3q}{(2\pi)^3} \mathcal{G}(q) \right)^2, \quad (\text{A6a})$$

$$\Gamma_2^{(2)} = \frac{\eta^2}{12N} \left[m \int \frac{d^3q_1 d^3q_2}{(2\pi)^6} \mathcal{G}(q_1) \mathcal{G}(q_2) \mathcal{G}(-q_1 - q_2) + \frac{m(m-1)}{2} \int \frac{d^3q_1 d^3q_2}{(2\pi)^6} \mathcal{F}(q_1) \mathcal{F}(q_2) \mathcal{F}(-q_1 - q_2) \right], \quad (\text{A6b})$$

$$\Gamma_2^{(4)} = \frac{\lambda^2}{48N^{3/2}} \left[m \int \frac{d^3q_1 d^3q_2 d^3q_3}{(2\pi)^9} \mathcal{G}(q_1) \mathcal{G}(q_2) \mathcal{G}(q_3) \mathcal{G}(-q_1 - q_2 - q_3) + \frac{m(m-1)}{2} \int \frac{d^3q_1 d^3q_2 d^3q_3}{(2\pi)^9} \mathcal{F}(q_1) \mathcal{F}(q_2) \mathcal{F}(q_3) \mathcal{F}(-q_1 - q_2 - q_3) \right]. \quad (\text{A6c})$$

Using the polarization functions $\Pi_{ab}(k)$ defined as

$$\begin{aligned} \Pi_{ab}(k) &= \int \frac{d^3q}{(2\pi)^3} G_{ab}(q) G_{ba}(k+q) \\ &= [\Pi_{\mathcal{G}}(k) - \Pi_{\mathcal{F}}(k)] \delta_{ab} + \mathcal{F}(k), \\ \Pi_{\mathcal{G}}(k) &= \int \frac{d^3q}{(2\pi)^3} \mathcal{G}(q) \mathcal{G}(k+q), \end{aligned} \quad (\text{A7a})$$

$$\Pi_{\mathcal{F}}(k) = \int \frac{d^3q}{(2\pi)^3} \mathcal{F}(q) \mathcal{F}(k+q). \quad (\text{A7b})$$

we can rewrite the self-energy functions after taking $m = 1$ as

$$\begin{aligned}\Sigma_{ab} &= (\Sigma_{\mathcal{G}} - \Sigma_{\mathcal{F}}) \delta_{ab} + \Sigma_{\mathcal{F}}, \\ \Sigma_{\mathcal{G}}(k) &= \frac{\lambda}{2\bar{N}^{1/2}} \int \frac{d^3q}{(2\pi)^3} \mathcal{G}(q) - \frac{\eta^2}{2\bar{N}^{1/2}} \Pi_{\mathcal{G}}(k) - \frac{\lambda^2}{6\bar{N}} \int \frac{d^3q}{(2\pi)^3} \mathcal{G}(q) \Pi_{\mathcal{G}}(q+k),\end{aligned}\quad (\text{A8a})$$

$$\Sigma_{\mathcal{F}}(k) = -\frac{\eta^2}{2\bar{N}^{1/2}} \Pi_{\mathcal{F}}(k) - \frac{\lambda^2}{6\bar{N}} \int \frac{d^3q}{(2\pi)^3} \mathcal{F}(q) \Pi_{\mathcal{F}}(q+k). \quad (\text{A8b})$$

The configurational entropy is obtained from Eqs. (33) and (A6) to be

$$\begin{aligned}S_c &= \frac{1}{T} \left. \frac{\partial F_m}{\partial m} \right|_{m=1} = S_c^{(0)} + S_c^{(1)}, \\ S_c^{(0)} &= -\frac{1}{2\bar{N}^{1/2}} \int \frac{d^3q}{(2\pi)^3} \left[\log \left(1 - \frac{\mathcal{F}(q)}{\mathcal{G}(q)} \right) - \frac{\mathcal{F}(q)}{\mathcal{G}(q)} \right],\end{aligned}\quad (\text{A9a})$$

$$S_c^{(1)} = -\frac{\eta^2}{24\bar{N}} \int \frac{d^3q}{(2\pi)^3} \Pi_{\mathcal{F}}(q) \mathcal{F}(-q) - \frac{\lambda^2}{96\bar{N}^{3/2}} \int \frac{d^3q}{(2\pi)^3} \Pi_{\mathcal{F}}(q) \Pi_{\mathcal{F}}(-q). \quad (\text{A9b})$$

We set $k_B = 1$.

APPENDIX B: ORDER-DISORDER TRANSITION

In this appendix, we present our calculation of the ODT in diblock-copolymer melts. Our approach is different from the Brazovskii approximation [18, 40]. Following the derivation in Appendix A, we expand the effective potential to two-loop order and keep only the diagonal terms in Eqs. (A4):

$$\begin{aligned}\Gamma[\bar{\phi} = \varphi] &= F_L(\varphi) + \frac{1}{2\bar{N}^{1/2}} \text{Tr} \log \mathcal{G}^{-1} + \frac{1}{2\bar{N}^{1/2}} \text{Tr}(D^{-1} \mathcal{G}) + \frac{\lambda}{8\bar{N}} \left[\int \frac{d^3q}{(2\pi)^3} \mathcal{G}(q) \right]^2 \\ &\quad - \frac{\eta^2}{12\bar{N}} \int \frac{d^3q}{(2\pi)^3} \mathcal{G}(q) \Pi_{\mathcal{G}}(-q) - \frac{\lambda^2}{12\bar{N}} \int \frac{d^3q_1 d^3q_2}{(2\pi)^6} \varphi(q_1) \mathcal{G}(q_2) \Pi_{\mathcal{G}}(q_1 + q_2) \varphi(-q_1),\end{aligned}\quad (\text{B1})$$

where $F_L(\varphi)$ is the Leibler free energy for the ordered phase, $D(q)$ is the shifted bare propagator as given in Eq. (10). The Hartree approximation (similar to the Brazovskii approximation) amounts to keeping only the terms in the first row of Eq. (B1), which can be justified by a renormalization-group argument [66]. The central idea is the following: since near the critical temperature the dominant fluctuations are those with wave numbers close to q_m at which the propagator is maximized, one can decompose the spherical shell into small ‘‘patches’’ and rewrite the order parameter into n components each corresponding to one patch. In this way one can rewrite the original Hamiltonian [Eq. (2)] as a $1/n$ model. At the critical point, n goes to infinity and the Hartree approximation becomes exact. Therefore we may replace \mathcal{G} by the Hartree approximation \mathcal{G}_H as defined in Eq. (13)

$$\mathcal{G}_H(k)^{-1} = D(k)^{-1} + \frac{\lambda}{2\bar{N}^{1/2}} \int \frac{d^3q}{(2\pi)^3} \mathcal{G}_H(q).$$

This gives the first three terms in Eq. (11).

However, here we want to study the correction due to the cubic coupling; thus we want to include the leading-order diagram from the cubic interaction in the effective potential, as shown in Fig. 5(b). It can be shown that in the corresponding n -vector model as mentioned above, the Hartree term [Fig. 5(a)] is of order $O(n)$ and this correction term [Fig. 5(b)] is of order $O(n^{1/2})$. By a similar argument the last term in Eq. (B1) is of order $O(1)$ and ignored in our calculation. Finally the free energy is given by Eq. (B1) with the last term dropped, which becomes Eq. (11). To find the ODT temperature, the free energy is minimized numerically with respect to the magnitude of density wave a as given in Eq. (8), and the ODT occurs when the free energy of the ordered phase equals the free energy of the disordered phase.

The physical correlation function is given by Eq. (14) and the corresponding self-energy is

$$\Sigma_{\mathcal{G}}(k) = \frac{\lambda}{2\bar{N}^{1/2}} \int \frac{d^3q}{(2\pi)^3} \mathcal{G}_H(q) - \frac{\eta^2}{6\bar{N}^{1/2}} \int \frac{d^3q}{(2\pi)^3} \mathcal{G}_H(q) \mathcal{G}_H(q+k). \quad (\text{B2})$$

This renormalization scheme includes two parts, the first corresponding to a simple Hartree approximation and the second incorporating fluctuations from the cubic interaction using the Hartree-renormalized propagator, which is schematically shown in the following diagrammatic equations:

$$\begin{aligned}
 \text{Double line} &= \text{Thin line} - \frac{\lambda}{2} \text{Loop}, \\
 \text{Thin line} &= \text{Double line} + \frac{\eta^2}{2} \text{Bubble},
 \end{aligned} \tag{B3}$$

where the thin lines represent the bare propagator $g(q)$, the double lines represent the Hartree-renormalized propagator $\mathcal{G}_H(q)$, and the thick lines are the physical propagator $\mathcal{G}(q)$. Eq. (B2) modifies the self-energy equation (A8a) we derived using a straightforward loop expansion in Appendix A. One can verify that this self-energy equation does not have the unphysical nonmonotonic relation between the temperature (manifested through χN in τ_0) and the correlation length (manifested in r in $\mathcal{G}(q)$) at low temperatures. Therefore we use Eq. (B2) as the diagonal self-energy in the replica calculation.

APPENDIX C: APPROXIMATE SOLUTIONS OF THE GLASS TRANSITIONS

In this last appendix we provide an approximate solution of the self-consistent equations obtained in Appendix A. The diagonal and off-diagonal self-energy equations are shown in the following diagrammatic equations:

$$\text{Circle} = -\frac{\lambda}{2} \text{Loop} + \frac{\eta^2}{2} \text{Bubble}, \tag{C1}$$

$$\text{Hatched Circle} = \frac{\eta^2}{2} \text{Dashed Loop} - \frac{\lambda^2}{6} \text{Dashed Bubble}, \tag{C2}$$

where the broken lines represent the renormalized off-diagonal propagator \mathcal{F} ; the thick lines and the double lines represent the renormalized diagonal propagator \mathcal{G} and the Hartree-renormalized propagator respectively, same as before.

From Eqs. (29) and (32) the renormalized propagators \mathcal{G} and \mathcal{F} are given by

$$\mathcal{G}(q) = \frac{4q_m^2}{(q^2/q_m^2 - 1)^2 + 4r}, \tag{29'}$$

$$\mathcal{F}(q) = \frac{4q_m^2}{(q^2/q_m^2 - 1)^2 + 4r} - \frac{4q_m^2}{(q^2/q_m^2 - 1)^2 + 4s}. \tag{32'}$$

When r, s are small, the polarization functions can be

approximated as

$$\Pi_{\mathcal{G}}(k) \simeq \frac{1}{4kr}, \tag{C3a}$$

$$\Pi_{\mathcal{F}}(k) \simeq \frac{1}{4k} \left(\frac{1}{\sqrt{r}} - \frac{1}{\sqrt{s}} \right)^2, \tag{C3b}$$

for $0 < |k| < 2$ and zero elsewhere. These are verified numerically and work well for r, s not too large ($\lesssim 0.1$). The diagrammatic terms in our calculations are found to be

$$\int \frac{d^3q}{(2\pi)^3} \mathcal{G}(q) \approx \frac{1}{2\pi\sqrt{r}} \tag{C4a}$$

$$\int \frac{d^3q}{(2\pi)^3} \mathcal{G}(k-q) \Pi_{\mathcal{G}}(q) \Big|_{k=q_m} \approx \frac{1}{8\pi r \sqrt{r}}, \tag{C4b}$$

$$\int \frac{d^3q}{(2\pi)^3} \mathcal{F}(k-q) \Pi_{\mathcal{F}}(q) \Big|_{k=q_m} \approx \frac{1}{8\pi} \left(\frac{1}{\sqrt{r}} - \frac{1}{\sqrt{s}} \right)^3, \quad (\text{C4c})$$

$$\int \frac{d^3q}{(2\pi)^3} \mathcal{F}(-q) \Pi_{\mathcal{F}}(q) \approx \frac{1}{2\pi} \left(\frac{1}{\sqrt{r}} - \frac{1}{\sqrt{s}} \right)^3, \quad (\text{C4d})$$

$$\int \frac{d^3q}{(2\pi)^3} \Pi_{\mathcal{F}}(-q) \Pi_{\mathcal{F}}(q) \approx \frac{1}{2\pi^2} \left(\frac{1}{\sqrt{r}} - \frac{1}{\sqrt{s}} \right)^4. \quad (\text{C4e})$$

From Eqs. (B3) and (29') we have the following equations for r

$$\tau_0 = \tau - \frac{\lambda}{4\pi \bar{N}^{1/2} q_m \sqrt{\tau}}, \quad (\text{C5})$$

$$r = \tau - \frac{\eta^2}{8\pi \bar{N}^{1/2} q_m^3 \tau}.$$

And from Eqs. (C2) and (32') we have

$$s - r = \frac{\lambda^2}{48\pi \bar{N} q_m^2} \left(\frac{1}{\sqrt{r}} - \frac{1}{\sqrt{s}} \right)^3 + \frac{\eta^2}{8\bar{N}^{1/2} q_m^3} \left(\frac{1}{\sqrt{r}} - \frac{1}{\sqrt{s}} \right)^2. \quad (\text{C6})$$

Let's look at Eq. (C6) first. Define $t \equiv \sqrt{r/s}$, Eq. (C6) becomes

$$t^{-2} - 1 = \frac{\lambda^2(1-t)^3}{48\pi \bar{N} q_m^2 r^{5/2}} + \frac{\eta^2(1-t)^2}{8\bar{N}^{1/2} q_m^3 r^2}. \quad (\text{C7})$$

This equation always has a replica-symmetric solution $t = 1$ ($\mathcal{F} = 0$.) Here we are seeking a replica-symmetry-broken solution with $t < 1$. Define the dimensionless parameters

$$A \equiv \frac{\lambda^2}{48\pi \bar{N} q_m^2 r^{5/2}},$$

$$B \equiv \frac{\eta^2}{8\bar{N}^{1/2} q_m^3 r^2}.$$

Eq. (C7) becomes

$$\frac{A(1-t)^2 t^2}{1+t} + \frac{B(1-t)t^2}{1+t} = 1. \quad (\text{C7}')$$

Numerical calculations show that when both A and B are non-negative and either $A > 23.66$ or $B > 11.09$, there is always a solution $0 < t^* < 1$. For symmetric copolymer and very asymmetric copolymer respectively, these inequalities result in the following criteria

$$r \lesssim \left(\frac{\lambda^2}{\bar{N} q_m^2} \right)^{2/5} \sim \bar{N}^{-2/5}, \quad (\text{C8})$$

$$r \lesssim \left(\frac{\eta^2}{\bar{N}^{1/2} q_m^3} \right)^{1/2} \sim \bar{N}^{-1/4}. \quad (\text{C9})$$

And the resulted scaling relations for τ_0 [$\propto (\chi N)_S - \chi N$] for symmetric and asymmetric copolymers are respectively

$$\tau_0 \sim -\bar{N}^{-0.3}, \quad (\text{C10})$$

$$\tau_0 \sim \bar{N}^{-1/4}. \quad (\text{C11})$$

These have been verified by our numerical calculations.

Finally we look at the configurational entropy and the Kauzmann temperature. The configurational entropy is given in Eqs. (A9) and found to be

$$S_c^{(0)} = \frac{q_m^3 \sqrt{r}}{4\pi \bar{N}^{1/2} t} (1-t)^2, \quad (\text{C12a})$$

$$S_c^{(1)} \approx -\frac{\eta^2}{96\pi \bar{N} r^{3/2}} (1-t)^3 - \frac{\lambda^2 q_m}{1536\pi^2 \bar{N}^{3/2} r^2} (1-t)^4. \quad (\text{C12b})$$

Thus for symmetric copolymer ($\eta = 0$), the Kauzmann transition is located at

$$r \sim \bar{N}^{-2/5}, \quad (\text{C13})$$

$$\tau_0 \sim -\bar{N}^{-0.3}. \quad (\text{C14})$$

And for very asymmetric copolymer ($\eta/q_m^{3/2} \gg \lambda/q_m$)

$$r \sim \bar{N}^{-1/4}, \quad (\text{C15})$$

$$\tau_0 \sim \bar{N}^{-1/4}. \quad (\text{C16})$$

-
- [1] I. W. Hamley, *The Physics of Block Copolymers* (Oxford University Press, 1998).
 [2] I. W. Hamley, ed., *Developments in Block Copolymer Science and Technology* (John Wiley and Sons, Ltd, 2004).
 [3] F. S. Bates and G. H. Fredrickson, *Annu. Rev. Phys. Chem.* **41**, 525 (1990).
 [4] F. S. Bates and G. H. Fredrickson, *Phys. Today* **52**, 32

- (1999).
 [5] F. S. Bates, M. F. Schulz, A. K. Khandpur, S. Förster, and J. H. Rosedale, *Faraday Discuss.* **98** (1994).
 [6] F. S. Bates, R. E. Cohen, and C. V. Berney, *Macromolecules* **15**, 589 (1982).
 [7] S. P. Gido and E. L. Thomas, *Macromolecules* **27**, 6137 (1994).

- [8] F. S. Bates, J. H. Rosedale, and G. H. Fredrickson, *J. Chem. Phys.* **92**, 6255 (1990).
- [9] K. Almdal and F. S. Bates, *J. Chem. Phys.* **96**, 9122 (1992).
- [10] J. H. Rosedale and F. S. Bates, *Macromolecules* **23**, 2329 (1990).
- [11] M. W. Matsen and M. Schick, *Phys. Rev. Lett.* **72**, 2660 (1994).
- [12] M. W. Matsen and F. S. Bates, *Macromolecules* **29**, 1091 (1996).
- [13] J. G. E. M. Fraaije, B. A. C. van Vlimmeren, N. M. Maurits, and M. Postma, *J. Chem. Phys.* **106**, 4260 (1996).
- [14] N. M. Maurits, B. A. C. van Vlimmeren, and J. G. E. M. Fraaije, *Phys. Rev. E* **56**, 816 (1997).
- [15] N. P. Balsara, B. A. Garetz, M. C. Newstein, B. J. Bauer, and T. J. Prosa, *Macromolecules* **31**, 7668 (1998).
- [16] W. G. Kim, M. Y. Chang, B. A. Garetz, M. C. Newstein, N. P. Balsara, J. H. Lee, H. Han, and S. S. Patel, *J. Chem. Phys.* **114**, 10196 (2001).
- [17] D. J. Pochan, S. P. Gido, S. Pispas, and J. W. Mays, *Macromolecules* **29**, 5099 (1996).
- [18] G. H. Fredrickson and E. Helfand, *J. Chem. Phys.* **87**, 697 (1987).
- [19] L. Leibler, *Macromolecules* **13**, 1602 (1980).
- [20] J. L. Adams, W. G. Graessley, and R. A. Register, *Macromolecules* **27**, 6026 (1994).
- [21] J. L. Adams, D. J. Quiram, W. W. Graessley, R. A. Register, and G. R. Marchand, *Macromolecules* **29**, 2929 (1996).
- [22] M. Schwab and B. Stühn, *Phys. Rev. Lett.* **76**, 924 (1996).
- [23] J. K. Kim, H. H. Lee, S. Sakurai, S. Aida, J. Masamoto, S. Nomura, Y. Kitagawa, and Y. Suda, *Macromolecules* **32**, 6707 (1999).
- [24] C. D. Han, N. Y. Vaidya, D. Kim, G. Shin, D. Yamaguchi, and T. Hashimoto, *Macromolecules* **33**, 3767 (2000).
- [25] N. Sota, N. Sakamoto, K. Saijo, and T. Hashimoto, *Macromolecules* **36**, 4534 (2003).
- [26] S. Choi, K. M. Lee, C. D. Han, N. Sota, and T. Hashimoto, *Macromolecules* **36**, 793 (2003).
- [27] X. Wang, E. E. Dormidontova, and T. P. Lodge, *Macromolecules* **35**, 9687 (2002).
- [28] A. N. Semenov, *Macromolecules* **22**, 2849 (1989).
- [29] E. E. Dormidontova and T. P. Lodge, *Macromolecules* **34**, 9143 (2001).
- [30] J. Wang, Z.-G. Wang, and Y. Yang, *Macromolecules* (2005), available through ASAP.
- [31] R. Monasson, *Phys. Rev. Lett.* **75**, 2847 (1995).
- [32] Z. Nussinov, J. Rudnick, and S. A. Kivelson, *Phys. Rev. Lett.* **83**, 472 (1999).
- [33] M. Mézard and G. Parisi, *J. Phys:Condens. Matter* **12**, 6655 (2000).
- [34] B. Coluzzi, G. Parisi, and P. Verrocchio, *Phys. Rev. Lett.* **84**, 306 (2000).
- [35] J. Schmalian and P. G. Wolynes, *Phys. Rev. Lett.* **85**, 836 (2000).
- [36] H. Westfahl, Jr., J. Schmalian, and P. G. Wolynes, *Phys. Rev. B* **64**, 174203(16) (2001).
- [37] S. Wu, J. Schmalian, G. Kotliar, and P. G. Wolynes, *Phys. Rev. B* **70**, 024207 (2004).
- [38] P. G. Debenedetti and F. H. Stillinger, *Nature* **410**, 259 (2001).
- [39] S. Wu, H. W. Jr., J. Schmalian, and P. G. Wolynes, *Chem. Phys. Lett.* **359**, 1 (2002).
- [40] S. A. Brazovskii, *Zh. Exp. Theor. Fiz. JETP* **68**, 175 (1975).
- [41] M. Grousson, V. Krakoviack, G. Tarjus, and P. Viot, *Phys. Rev. E* **66**, 026126 (2002).
- [42] M. O. de la Cruz, *Phys. Rev. Lett.* **67**, 85 (1991).
- [43] A. V. Dobrynin and I. Y. Erukhimovich, *J. Phys. II France* **11**, 1387 (1991).
- [44] J.-L. Barrat and G. H. Fredrickson, *J. Chem. Phys.* **95**, 1281 (1991).
- [45] T. Ohta and K. Kawasaki, *Macromolecules* **19**, 2621 (1986).
- [46] L. Kielhorn and M. Muthukumar, *J. Chem. Phys.* **107**, 5588 (1997).
- [47] A. Kudlay and S. Stepanow, *J. Chem. Phys.* **118**, 4272 (2003).
- [48] Z.-G. Wang, *J. Chem. Phys.* **117**, 481 (2002).
- [49] J. M. Cornwall, R. Jackiw, and E. Tomboulis, *Phys. Rev. D* **10**, 2428 (1974).
- [50] W. Götze, *Liquids, Freezing and Glass Transition (Part I)* (North-Holland, 1989), chap. 5. Aspects of structural glass transitions, Les Houches LI.
- [51] S. F. Edwards and P. W. Anderson, *J. Phys. F* **6**, 1927 (1976).
- [52] Y. Singh, J. P. Stoessel, and P. G. Wolynes, *Phys. Rev. Lett.* **54**, 1059 (1985).
- [53] M. Mézard, G. Parisi, and M. A. Virasoro, eds., *Spin Glass Theory and Beyond*, Lecture Notes in Physics Vol. 9 (World Scientific, 1987).
- [54] T. R. Kirkpatrick and P. G. Wolynes, *Phys. Rev. A* **35**, 3072 (1987).
- [55] W. Kauzmann, *Chem. Rev.* **43**, 219 (1948).
- [56] M. Grousson, G. Tarjus, and P. Viot, *Phys. Rev. E* **64**, 036109 (2001).
- [57] M. Grousson, G. Tarjus, and P. Viot, *Phys. Rev. E* **65**, 065103 (2002).
- [58] P. L. Geissler and D. R. Reichman, *Phys. Rev. E* **69**, 021501(9) (2004).
- [59] Z. Nussinov, *Phys. Rev. B* **69**, 014208 (2004).
- [60] D. D. Ling, B. Friman, and G. Grinstein, *Phys. Rev. B* **24**, 2718 (1981).
- [61] P. C. Hohenberg and J. B. Swift, *Phys. Rev. A* **52**, 1828 (1995).
- [62] W. L. Johnson, *Mat. Res. Bull.* **24**, 42 (1999).
- [63] X. Xia and P. G. Wolynes, *Proc. Natl. Aca. Sci.* **97**, 2990 (2000).
- [64] C. A. Angell, *Science* **267**, 1924 (1995).
- [65] J. Schmalian, S. Wu, and P. G. Wolynes (2003), cond-mat/03054201.
- [66] R. Shankar, *Rev. Mod. Phys.* **66**, 129 (1994).
- [67] Indeed, treating the disordered spherical micelles as large localized fluctuations using the Hamiltonian [Eq. (1)] as the density functional, we can reproduce results similar to those obtained by Wang *et al.* using the self-consistent-field method [30]. We find that the cubic term is largely responsible for the appearance of the disordered micelles. Unpublished
- [68] C.-Z. Zhang and Z.-G. Wang, unpublished
- [69] For a discussion on the possible differences between polycrystalline phases and structural glasses, see Ref. [37].